First-order phase transitions in classical lattice gas spin models

H. Chamati
Institute of Solid State Physics, Bulgarian Academy of Sciences, 72 Tzarigradsko Chaussée, 1784 Sofia, Bulgaria

S. Romano
Unitá di Ricerca CNISM e Dipartimento di Fisica "A. Volta," Universitá di Pavia, via A. Bassi 6, I-27100 Pavia, Italy
(Received 13 January 2007; published 14 May 2007)

The present paper considers some classical ferromagnetic lattice-gas models, consisting of particles that carry n-component spins ($n=2,3$) and associated with a D-dimensional lattice ($D=2,3$); each site can host one particle at most, thus implicitly allowing for hard-core repulsion; the pair interaction, restricted to nearest neighbors, is ferromagnetic, and site occupation is also controlled by the chemical potential μ. The models had previously been investigated by mean field and two-site cluster treatments (when $D=3$), as well as grand-canonical Monte Carlo simulation in the case $\mu=0$, for both $D=2$ and $D=3$; the obtained results showed the same kind of critical behavior as the one known for their saturated lattice counterparts, corresponding to one particle per site. Here we addressed by grand-canonical Monte Carlo simulation the case where the chemical potential is negative and sufficiently large in magnitude; the value $\mu=-D/2$ was chosen for each of the four previously investigated counterparts, together with $\mu=-3D/4$ in an additional instance. We mostly found evidence of first-order transitions, both for $D=2$ and $D=3$, and quantitatively characterized their behavior. Comparisons are also made with recent experimental results.

DOI: 10.1103/PhysRevB.75.184413 PACS number(s): 75.10.Hk, 05.50.+q, 64.60.−i

I. INTRODUCTION

There exist a few statistical mechanical models involving classical continuous spins, by now extensively investigated, and which play a central role in a variety of real physical situations; they have been especially studied in their saturated lattice (SL) version, where each lattice site hosts one spin. The interest in their lattice gas (LG) extensions was recently revived, and they were addressed by means of analytical theories and simulation (see, for example, Refs. 1–8 and references therein). LG spin models are obtained from their SL counterparts by allowing for fluctuations of occupation numbers, also controlled by the chemical potential μ. These models have often been used in connection with alloys and absorption; the methodology somehow allows for pressure and density effects.

As for symbols and definitions, classical SL spin models involve n-component unit vectors $\mathbf{u}_k$, associated with a D-dimensional (bipartite) lattice $\mathbb{Z}^D$; let $\mathbf{x}_k$ denote dimensionless coordinates of the lattice sites, and let $u_{k,\alpha}$ denote Cartesian spin components with respect to an orthonormal basis $\mathbf{e}_\alpha$, whose unit vectors can be taken as defined by the lattice axes. The orientations of the magnetic moments of the particles are parametrized by usual polar angles $\{\phi_j\}$ ($n=2$) or spherical ones $\{(\varphi_j,\theta_j)\}$ ($n=3$). The interaction potential, restricted to nearest neighbors, is assumed to be ferromagnetic and, in general, anisotropic in spin space, i.e.,

$$\Phi_{jk}=\epsilon Q_{jk},\quad Q_{jk}=-\left(au_{j,n}u_{k,n}+b\sum_{\alpha<n}u_{j,\alpha}u_{k,\alpha}\right),\quad \epsilon>0,$$

$$a\geqslant 0,\quad b\geqslant 0,\quad a+b>0,\quad \max(a,b)=1. \tag{1}$$

Notice also that the condition $\max(a,b)=1$ in the above equation can always be satisfied by a suitable rescaling of ϵ; here and in the following the quantity ϵ will be used to set temperature and energy scales; thus $T=k_Bt/\epsilon$, where t denotes the absolute temperature and k_B is the Boltzmann constant; the corresponding (scaled) Hamiltonian is given by

$$\Lambda=\sum_{\{j<k\}}Q_{jk}. \tag{2}$$

The case $n=1$ corresponds to the Ising model; isotropic $O(n)$-symmetric models ($n>1$) correspond to $a=b$, $Q_{jk}=-\mathbf{u}_j\cdot\mathbf{u}_k$, and are referred to as planar rotators (PR, $n=2$) or classical Heisenberg model (He, $n=3$); the extremely anisotropic and $O(2)$-symmetric XY model is defined by $n=3$, $a=0$. For these models the simplification resulting from the neglect of translational degrees of freedom makes it possible to obtain rigorous mathematical results[9–11] entailing existence or absence of a phase transition, and, on the other hand, to study it by a whole range of techniques, such as mean field (MF) and cluster mean field treatments, high-temperature series expansion of the partition function, renormalization group (for a recent review see Ref. 12), computer simulation [usually via Monte Carlo (MC) methods[13]].

LG extensions of the continuous-spin potential model considered here are defined by Hamiltonians

$$\Lambda=\sum_{\{j<k\}}\nu_j\nu_k(\lambda-\Omega_{jk})-\mu N,\quad N=\sum_k\nu_k, \tag{3}$$

where $\nu_k=0,1$ denotes occupation numbers; notice that $\lambda\leqslant 0$ reinforces the orientation-dependent term, whereas $\lambda>0$ opposes it, and that a finite value of λ only becomes immaterial in the SL limit $\mu\to+\infty$. It is worth mentioning that in such systems the fluctuating occupation numbers give rise to additional fluidlike observables in comparison to the usual SL situation.

Rigorous results entailing existence or absence of an ordering transition are also known for LG models with con-

tinuous spins.[14–18] For some models defined by $D=3$, interactions isotropic in spin space, and supporting a ferromagnetic phase transition in their SL version, it has been proven that there exists a μ_0, such that, for all $\mu>\mu_0$, the system supports a ferromagnetic transition, with a μ-dependent transition temperature. Notice that $\mu_0<0$ when $\lambda\leqslant 0$,[15–17] whereas a positive μ_0 may be needed when $\lambda>0$. More recently,[18] the existence of a first-order transition, involving discontinuities in both density and magnetization, has been proven for the isotropic case (and $D=3$), in a suitable régime of low temperature and negative μ.

For $D=2$, the SL-PR model produces at low-temperature the extensively studied Berezinskiĭ-Kosterlitz-Thouless (BKT) transition;[19,20] the existence of such a transition for the LG counterpart has been proven rigorously as well.[21] More recently, it was rigorously proven[22] that, for μ negative and sufficiently large in magnitude, the transition becomes first order.

Notice also that the above mathematical theorems do not yield useful numerical estimates of the μ value where the change of transition sets in; some answer to this question can be looked for by analytical approximations such as MF or two-side-cluster (TSC) treatments,[3,5] or by simulation.[3,5,8]

The Hamiltonian [Eq. (3)] can be interpreted as describing a two-component system consisting of interconverting "real" ($\nu_k=1$) and "ghost," "virtual" or ideal-gas particles ($\nu_k=0$); both kinds of particles have the same kinetic energy, μ denotes the excess chemical potential of "real" particles over "ideal" ones, and the total number of particles equals the number of available lattice sites (semi-grand-canonical interpretation). The semi-grand-canonical interpretation was also used in early studies of the phase diagram of the two-dimensional planar rotator, carried out by the Migdal-Kadanoff RG techniques, and aiming at two-dimensional mixtures of ^{3}He and ^{4}He,[23,24] where nonmagnetic impurities correspond to ^{3}He.

In the three-dimensional case, the topology of the phase diagram of the model (3) had been investigated by MF and TSC approximations for the Ising[2] as well as PR cases[3] in the presence of a magnetic field, and for He at zero magnetic field.[5] These investigations were later extended[6] to extremely anisotropic (Ising-like) two-dimensional LG models defined by $a=1$, $b=0$ in Eq. (1), and in the absence of a magnetic field as well. The studied models were found to exhibit a tricritical behavior, i.e., the ordering transition turned out to be of first order for μ below an appropriate threshold, and of second order above it. When the transition is of first order, the orientationally ordered phase is also denser than the disordered one. For the three-dimensional PR these finding were confirmed, recently, by simulation in connection with the phase diagram of He.[4] It has been found that, despite the simplicity of LG spin models, their predictions broadly agree with the ones obtained by means of more elaborate magnetic fluid models (see, e.g., Ref. 25 and references therein).

On the other hand, thermodynamic and structural properties had been investigated by means of grand-canonical Monte Carlo simulations as well,[3,5] for particular values of the chemical potential equal or close to zero. It had been found that there is a *second order* ferromagnetic phase transition manifested by a significant growth of magnetic and density fluctuations. The transition temperatures were found to be about 20% lower than that of the corresponding SL values and the critical behavior of the investigated models to be consistent with that of their SL counterparts. Furthermore it had been found that MF yields a qualitatively correct picture, and the quantitative agreement with simulation could be improved by TSC, which has the advantage of predicting two-site correlations.

Notice also that the above Hamiltonian [Eq. (3)] describes a situation of *annealed* dilution; on the other hand, two-dimensional models in the presence of *quenched* dilution, and hence the effect of disorder on the BKT transition, have been investigated using the PR model[26–31] and very recently its *XY* counterpart;[31] it was found that a sufficiently weak disorder does not destroy the transition, which survives up to a concentration of vacancies close to the percolation threshold. Let us also remark that two-component spins are involved in the PR case, whereas *XY* involves three-component spins but only two of their components are involved in the interaction: in this sense the two models entail different anchorings with respect to the horizontal plane in spin space. Two-dimensional annealed lattice models were investigated[8] as well, and the obtained results for $\mu=0$ or a moderately negative μ were found to support those obtained for quenched models. For a large negative μ, renormalization-group treatments had suggested[23,24] that the transition between the BKT and the paramagnetic phase is of first order.

In this paper, we present an extensive Monte Carlo study of some LG ferromagnetic models, where μ is negative and comparatively large in magnitude (notice that $\mu<-D$ would produce an empty ground state), in order to gain insights into their critical behavior and to check the impact of the chemical potential on their physical properties. On the other hand, for $D=3$, we will also test the MF or TSC approximations used to obtain the phase diagrams of Refs. 3 and 5. In keeping with our previous studies, the models are further simplified by choosing $\lambda=0$, i.e., no pure positional interactions. As for the values of the chemical potential, we choose $\mu=-D/2$ in the four cases corresponding to our previous investigations with $\mu=0$, and carried out additional simulations for $D=2$, PR and $\mu=-3D/4$, as explained below.

The rest of the paper is organized as follows: the simulation procedure is briefly explained in Sec. II, Sec. III analyzes the simulation results. Finally, the effects caused by the chemical potential on the nature of the transition are discussed in Sec. IV, which summarizes our results, and where some comparisons are made with a recent experimental work.

II. MONTE CARLO SIMULATIONS

A detailed treatment of grand-canonical simulations can be found in or via Refs. 1, 5, and 32; the method outlined here has already been used in our previous studies of other LG models.[3,5,6] Simulations were carried out on periodically repeated samples, consisting of $V=L^D$ sites, where $L=40,80,120,160$ for $D=2$, and $L=10,20,30$ for $D=3$, i.e., in keeping with the named previous studies of ours; calcula-

tions were carried out in cascade, in order of increasing reduced temperature T.

The two basic MC steps used here were canonical and semi-grand-canonical attempts; in addition two other features were implemented:[33,34] (i) when a lattice site was visited, canonical or semi-grand-canonical steps were randomly chosen with probabilities $\mathcal{P}_{\rm can}$ and $\mathcal{P}_{\rm GC}$, respectively; we used $\mathcal{P}_{\rm can}/\mathcal{P}_{\rm GC}=n-1$, since spin orientation is defined by $(n-1)$ angles versus one occupation number and (ii) sublattice sweeps (checkerboard decomposition);[33,34] thus each sweep (or cycle) consisted of $2V$ attempts, first V attempts where the lattice sites were chosen randomly, then $V/2$ attempts on lattice sites of odd parity, and finally $V/2$ attempts on lattice sites of even parity. Equilibration runs took between 25 000 and 200 000 cycles, and production runs took between 250 000 and 1 000 000; macrostep averages for evaluating statistical errors were taken over 1000 cycles. Different random-number generators were used, as discussed in Ref. 34.

Computed thermodynamic observables included mean Hamiltonian per site, $H=(1/V)\langle\Lambda\rangle$, density $\rho=(1/V)\langle N\rangle$, as well as their derivatives with respect to temperature or chemical potential, $C_{\mu V}/k_B=(1/V)(\partial\langle\Lambda\rangle/\partial T)_{\mu,V}$, $\rho_T=(\partial\rho/\partial T)_{\mu,V}$, $\rho_\mu=(\partial\rho/\partial\mu)_{T,V}$, defined by appropriate fluctuation formulas.[32]

We also calculated mean magnetic moment per site and susceptibility, defined by

$$M=\frac{1}{V}\langle\sqrt{\mathbf{F}\cdot\mathbf{F}}\rangle, \tag{4}$$

where for PR or He the vector $\mathbf{F}$ is defined by

$$\mathbf{F}=\sum_{k=1}^{V}\nu_k\mathbf{u}_k, \tag{5}$$

whereas only the in-plane components of the vector spins (i.e., only the Cartesian components explicitly involved in the interaction potential) are accounted for in the XY case.

The behavior of the susceptibility was investigated by considering the two quantities

$$\chi_1=\frac{\beta}{V}(\langle\mathbf{F}\cdot\mathbf{F}\rangle-\langle|\mathbf{F}|\rangle^2) \tag{6}$$

and

$$\chi_2=\frac{\beta}{V}\langle\mathbf{F}\cdot\mathbf{F}\rangle; \tag{7}$$

simulation estimates of the susceptibility[13,35,36] are defined by

$$\chi=\begin{cases}\chi_1 & \text{in the ordered region,}\\ \chi_2 & \text{in the disordered region;}\end{cases} \tag{8}$$

notice also that, for a finite sample, $\chi_2\leqslant\beta V$, and that $\chi=\chi_2$ in two-dimensional cases.

A sample of V sites contains DV distinct nearest-neighboring pairs of lattice sites; we worked out pair occupation probabilities, i.e., the mean fractions R_{JK} of pairs being both empty $[R_{ee}=\langle(1-\nu_j)(1-\nu_k)\rangle]$, both occupied $[R_{oo}=\langle\nu_j\nu_k\rangle]$, or consisting of an empty and an occupied site $[R_{eo}=\langle(1-\nu_j)\nu_k+(1-\nu_k)\nu_j\rangle]$. It should be noted that $R_{ee}+R_{oo}+R_{eo}=1$.

Short- and long-range positional correlations were compared by means of the excess quantities

$$R'_{oo}=\ln\left(\frac{R_{oo}}{\rho^2}\right),\quad R''_{oo}=R_{oo}-\rho^2, \tag{9}$$

collectively denoted by R^*_{oo} (notice that these two definitions entail comparable numerical values).

Quantities such as ρ, ρ_T, ρ_μ and the above pair correlations R_{JK} or R^*_{oo} can be defined as "fluidlike," in the sense that they all go over the trivial constants in the SL limit. Let us also remark[8] that some of the above definitions (e.g., $C_{\mu,V}$ and ρ_T) involve the total potential energy both in the stochastic variable and in the probability measure ("explicit" dependence), whereas some other definitions, e.g., ρ_μ or the quantities R_{JK}, involve the total potential energy only in the probability measure ("implicit" dependence).

III. SIMULATION RESULTS

A. $D=2$, PR, $\mu=-1$

Simulation results, obtained in the named cases for a number of observables, such as the mean energy per site and density, showed that these quantities evolve with the temperature in a smooth way, and were found to be independent of sample sizes. In comparison with Ref. 8, their temperature derivatives $C_{\mu,V}$ and ρ_T (Fig. 1) showed recognizably more pronounced peaks about the same temperature $T\approx0.51$, around which the sample size dependence of results became slightly more pronounced. Comparison with our previous results shows that the location of the maximum of $C_{\mu V}$ is shifted towards lower temperatures as $\mu<0$ grows in magnitude.

Plots of $\ln\chi_2$ versus T, reported in Fig. 2, show results independent of sample size for $T\gtrsim0.52$, and then their pronounced increase with sample size for $T\lesssim0.51$, suggesting its divergence with L. In general this case *qualitatively* reproduces our previous simulation results,[8] but with more pronounced derivatives and peaks at a lower temperature. In order to estimate the critical temperature we applied the finite size scaling analysis, along the lines discussed in Ref. 8, and here again we found a BKT transition occurring at $T_{\rm BKT}=0.502\pm0.002$, corresponding to a particle density about 0.832 ± 0.003. Comparison between our previous results and the present ones shows that both transition temperature and "critical" particle concentration are monotonically increasing with the chemical potential (see Table I).

For the SL-PR model the maximum of the specific heat is located at about 15% (Ref. 37) above the BKT transition; for the LG-PR model and $\mu=0$ (Ref. 8) we had found a broad peak about 5% above the BKT transition, and here we find a sharper one about 2% above the transition temperature.

For $\mu=-1$, fluidlike quantities show qualitatively similar behaviors as their counterparts obtained for $\mu=0$. Results for ρ_T and ρ_μ, obtained with the largest sample sizes are reported in Fig. 1; they were found to behave in a similar fashion to

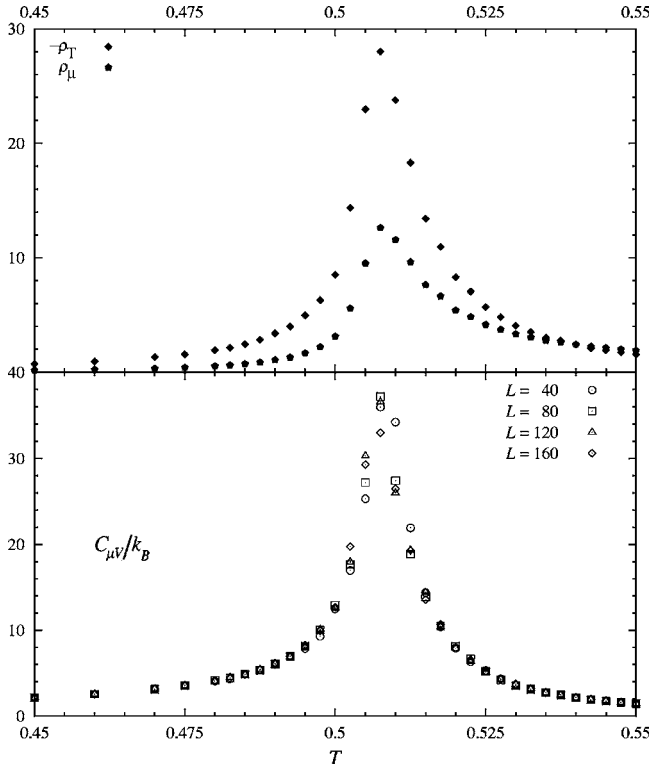

FIG. 1. Simulation estimates for the specific heat per site $C_{\mu V}$ versus temperature, obtained with different sample sizes, for the two-dimensional LG-PR and $\mu=-1$. Simulation results for ρ_T and ρ_μ obtained with the largest examined sample size are shown on the top. Statistical errors range between 1% and 5%.

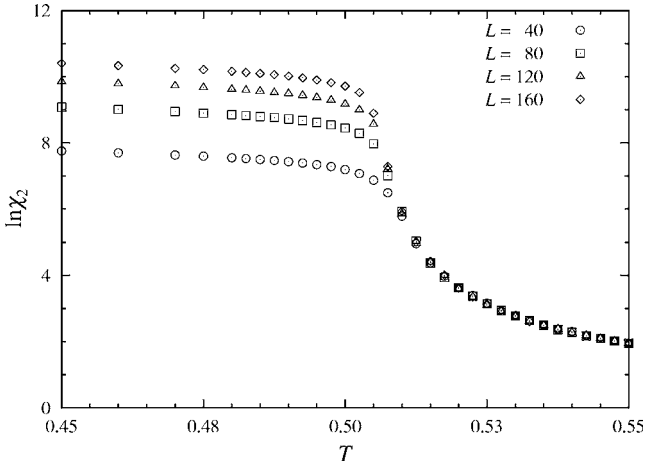

FIG. 2. Simulation estimates for the logarithm of the magnetic susceptibility χ_2 versus temperature, obtained with different sample sizes, for the two-dimensional LG-PR and $\mu=-1$. Unless otherwise stated, here and in the following figures, statistical errors fall within symbol sizes.

the specific heat and to exhibit sharper peaks taking place at the same temperature as that of $C_{\mu V}$. Recall that ρ_μ has a broad maximum for $\mu=0$. In other words, here the ferromagnetic orientational fluctuations taking place in the transition range do produce stronger fluctuations of site occupation variables, and this tends to reduce the difference between "implicit" and "explicit" dependencies on the potential energy as mentioned in Ref. 8.

Pair occupation probabilities R_{JK} were found to be insensitive to sample sizes; results for our largest sample size are shown in Fig. 3. These quantities are monotonic functions of temperature as their counterparts for $\mu=0$, but with more rapid variations across the transition region, in accordance with the sharper maximum of ρ_μ. Their behaviors suggest inflection points roughly corresponding to the maximum of ρ_μ.

Short- and long-range positional correlations have been compared via the excess quantities R^*_{oo}, whose simulation results for the largest sample size are shown in Fig. 4, showing sharper maxima than their counterparts corresponding to $\mu=0$. Notice also that the position of the maximum for R''_{oo} again corresponds to the location of the peak of $C_{\mu V}$. The quantities R^*_{oo} are rather small, and this could be traced back to the absence of pure positional interactions.

B. $D=2$ and first-order transitions

Additional simulations carried out for $D=2$, PR, $\mu=-3D/4$, showed a recognizably different scenario. Here, for all investigated sample sizes, we found pronounced jumps of

TABLE I. Transition temperatures Θ and "critical" particle density ρ_c of PR and XY models for some selected values of the chemical potential μ. Depending on μ we have either a BKT or a first-order transition (I); here ρ_c denotes the density at the BKT transition temperature.

Model	μ	Transition	Θ	ρ_c
PR($n=2$)	∞	BKT	0.907±0.004 (Ref. 31)	1.0
	0.1	BKT	0.75±0.01 (Ref. 8)	0.938±0.002
	0.0	BKT	0.733±0.003 (Ref. 8)	0.924±0.003 [8]
	−0.2	BKT	0.71±0.01 (Ref. 8)	0.900±0.002
	−1.0	BKT	0.502±0.002	0.832±0.003
	−1.5	I	0.279±0.001	
XY($n=3$)	∞	BKT	0.700±0.005 (Ref. 31)	1.0
	0.0	BKT	0.574±0.003 (Ref. 8)	0.918±0.004 (Ref. 8)
	−1.0	I	0.333±0.001	

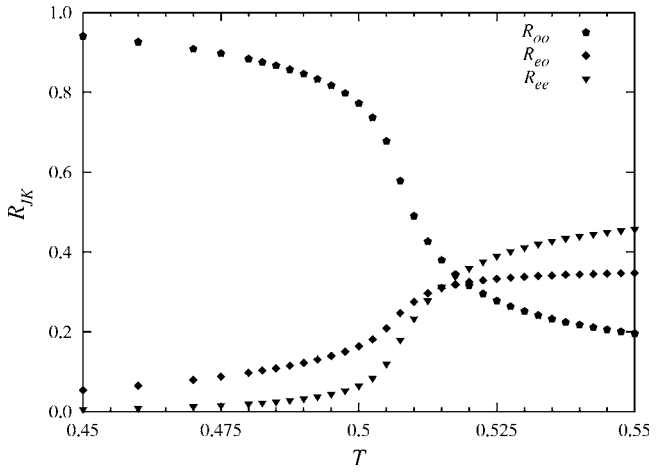

FIG. 3. Simulation estimates for the pair occupation probabilities R_{JK} versus temperature, for the two-dimensional LG-PR with linear sample size $L=160$. The results refer to $\mu=-1$.

various observables, such as H, ρ (Fig. 5) and even M (which kept decreasing with increasing sample size), taking place over a narrow temperature range, $\Delta T=0.0005$. Notice that χ_2 remains independent of sample sizes in the high-temperature regime, and then develops a pronounced increase with sample size. From a comparison of the behaviors of χ_2 for $\mu=-1$ (Fig. 2) and $\mu=-1.5$ (Fig. 7) one can observe the change of the critical behavior at the two values of μ. For $\mu=-1.5$ the thermodynamic observables show a discontinuous behavior characteristic of a first-order transition, now to a low-temperature BKT phase. The behaviors of $C_{\mu V}, \rho_T, \rho_\mu$ are shown in Fig. 6, and also exhibit pronounced differences from their counterparts in the previous case (see also below).

This result confirms previous RG predictions;[23,24] on the other hand, recent simulation studies addressing quenched dilution have found that the transition temperature vanishes below the percolation threshold.[28–31]

Notice that usage of the grand-canonical ensemble allows quite wide changes of density with temperature; in the investigated cases we used $\mu > -D$, and found that $\rho \approx 1$ in the

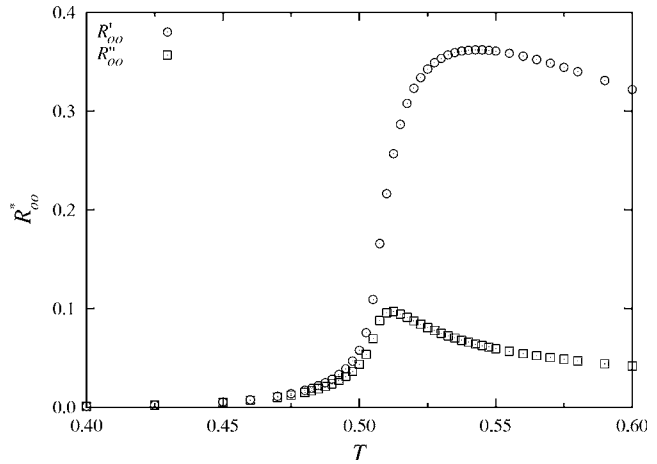

FIG. 4. Simulation estimates for the excess quantities R^*_{oo} for the two-dimensional LG-PR. Simulation results were obtained with $L=160$ and $\mu=-1$.

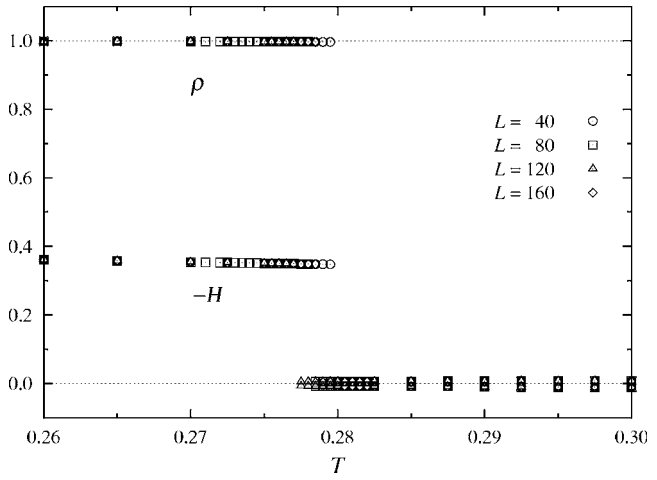

FIG. 5. Simulation results for the density ρ and the mean energy per site $-H$ obtained for the two-dimensional LG-PR. The value $\mu=-1.5$ was used for the present simulations.

low-T phase, where $\rho_T < 0$; such changes are obviously excluded from the start in the treatment of a quenched-dilution model. On the other hand, values $\mu < -D$ produce an essentially empty ground state; in this regime one can expect that ρ increases with T, only becoming appreciable above some threshold, and that the BKT phase disappears.

Here and in the following section, transitional properties such as ΔH, $\Delta \rho$ (as well as M, in the next section), were

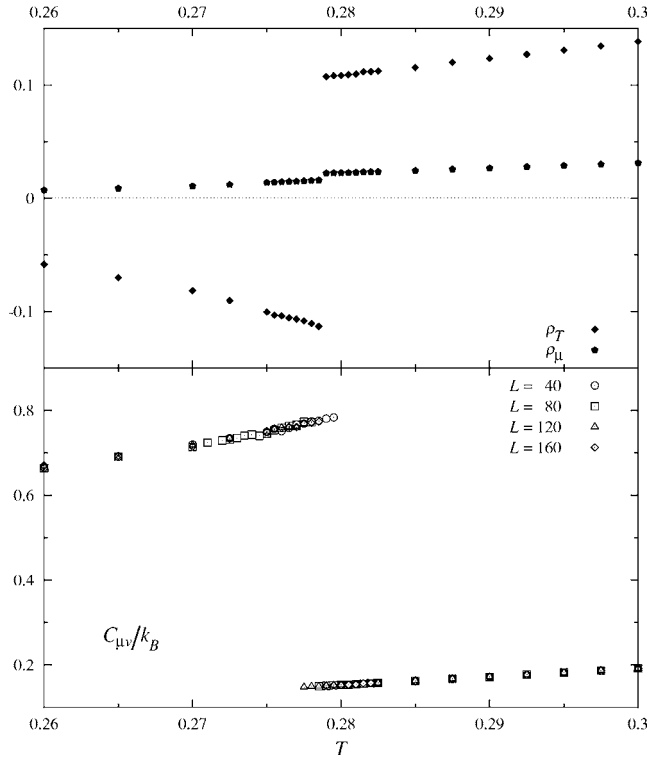

FIG. 6. Simulation estimates for the specific heat per site $C_{\mu V}$ versus temperature, obtained with different sample sizes for the two-dimensional LG-PR and $\mu=-1.5$. Simulation results for ρ_T and ρ_μ obtained with the largest examined sample size are shown on the top. Statistical errors range between 1% and 5%.

TABLE II. A summary of simulation estimates for properties at first-order transition for the two-dimensional models obtained using simulations.

Model	μ	Θ	ΔH	$\Delta\rho$
PR	−1.5	0.279±0.001	0.3562±0.0005	0.9917±0.0001
XY	−1.0	0.332±0.001	0.664±0.002	0.910±0.001

estimated by analyzing simulation results for the largest sample size as discussed in Refs. 38 and 39. The relevant results are reported in Table II.

Let us now turn to the discussion of the nature of the low-temperature phase. Here the magnetization was found to exhibit a power-law decay with increasing sample size. A fit to the expression

$$\ln M = -b_1 \ln L + b_0, \quad b_1 > 0, \tag{10}$$

showed that the ratio $b_1(T)/T$ is a constant. This shows that the magnetization goes to zero in the thermodynamic limit ($L \to \infty$), as predicted by the Mermin-Wagner theorem for two-dimensional (2D) systems, where no long-range order should survive. Note that this behavior is consistent with the spin-wave theory developed for the two-dimensional saturated planar rotator model.[37,40]

Results for $\ln \chi_2$ against temperature (Fig. 7) were found to be independent of sample size when $T \gtrsim 0.281$, and showed a recognizable increase with it (a linear dependence of $\ln \chi_2$ on $\ln L$) when $T \lesssim 0.278$. Thus in the low-temperature region the susceptibility exhibits a power law divergence with the linear sample size, showing a BKT phase.[37,40]

As for simulation results obtained for the *XY* LG model with $\mu=-1$, it was found that the thermodynamic quantities have qualitatively similar behaviors as those obtained for the above LG-PR with $\mu=-1.5$. The phase transition was found to be first order taking place at $T=0.332\pm0.001$; estimates of transition temperatures reported in Table I show that they

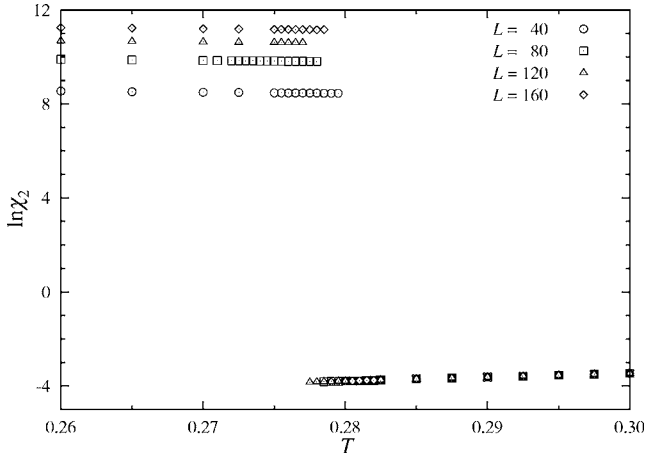

FIG. 7. Simulation estimates for the logarithm of the magnetic susceptibility χ_2 against temperature, obtained with different sample sizes for the two-dimensional LG-PR and $\mu=-1.5$.

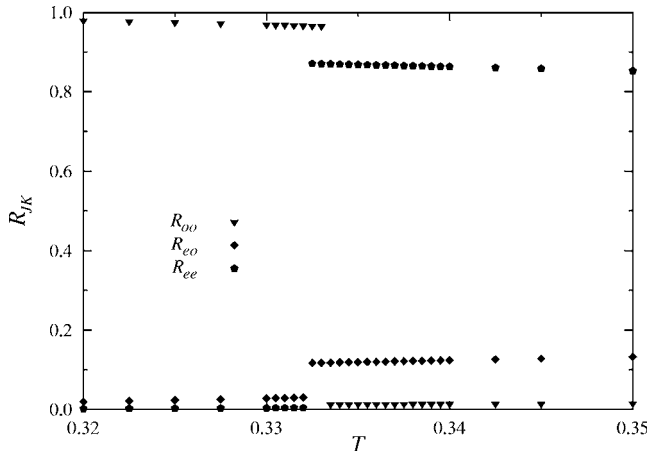

FIG. 8. Simulation estimates for the three pair occupation probabilities R_{JK}, for the two-dimensional LG-*XY*, for a sample with linear size $L=160$. The value $\mu=-1$ was used in this simulation.

increase as a function of the chemical potential. Transitional properties of the mean energy, the density, and the magnetization are presented in Table II. Here again we have found that the transition takes place from a paramagnetic to a BKT-like phase.

Let us emphasize that, as remarked above, PR and *XY* models entail different anchorings with respect to the horizontal plane in spin space; this difference correlates with the pronounced qualitative difference in transition behavior observed when $\mu=-1$.

When both PR and *XY* lattice gas models exhibited a first-order phase transition, their fluidlike quantities were found to behave in a qualitatively similar way. The following discussion will concentrate on these properties for the *XY* model.

Figure 6 shows that ρ_T is negative and decreases with increasing T in the low-temperature region (where it is essentially driven by orientational correlations), and then it becomes weakly positive and increasing with T in the high-temperature phase; thus, here and in the following section, ρ decreases with T in the low-temperature phase, and then increases with T in the high-temperature region. On the other hand, here ρ_μ is an increasing function of T, exhibiting a jump across the transition.

Simulation results for the pair occupation probabilities, reported in Fig. 8 and the excess quantities R^*_{oo} shown in Fig. 9, reveal that these quantities are discontinuous at the first-order transition region. On the other hand, they show the effects caused by the ferromagnetic interaction on the density in the system. The quantity R''_{oo} remains negligible due to the absence of purely positional interaction. The behavior of these quantities follows in general the trends of the mean Hamiltonian and the density. To summarize we found that the system exhibits a first-order phase transition from a dense BKT phase to a paramagnetic one; in the temperature-density phase diagram, both phases are expected to coexist over some range of densities and temperatures.

C. $D=3$ and first-order transitions

Simulation results presented in this section for the three-dimensional PR and He models show the effects caused by

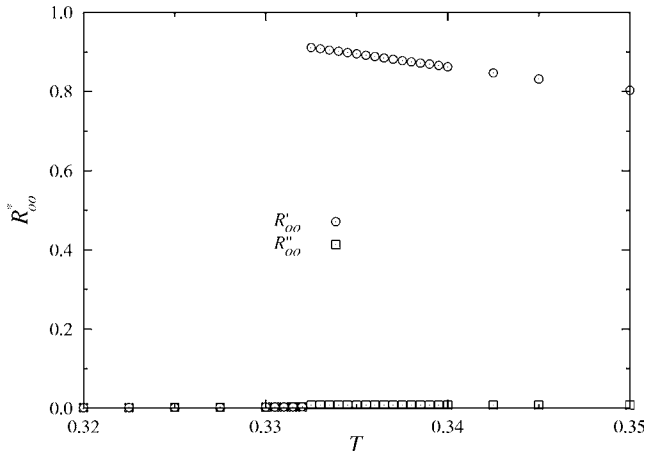

FIG. 9. Simulation estimates for the quantities R^*_{oo}, obtained with $L=160$ for the two-dimensional LG-XY and $\mu=-1$.

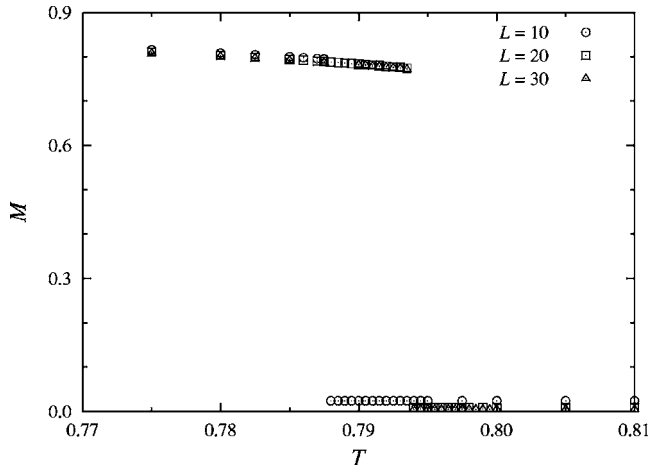

FIG. 10. Simulation results for the magnetization M against the temperature for the three-dimensional LG-PR, obtained with different sample sizes and $\mu=-1.5$.

large negative μ on their transitional behavior, and, on the other hand, can be used to check the predictions of the molecular-field-like treatments used to construct the phase diagrams reported in our previous papers;[3,5] we refer to them for further details, and present here only the final numerical results for the specific cases of interest.

It is well known that these approximate treatments do not describe fluctuations adequately, so that their predictions must be taken with caution. For example, MF predicted a first-order phase transition at $\mu=0$, while TSC and MC gave evidence of a second-order phase transition for He.[5] For both three-dimensional models, simulations performed for a selected value of the chemical potential, revealed that MF describes qualitatively well the transitional properties of the named models and that TSC improves upon it. In Table III we report results for the transition temperature obtained, via simulations, for some values of μ for these models so far. Here also one can read that the transition temperature decreases with decreasing μ.

Simulation results for both models exhibited a recognizable qualitative similarity, so that only plots of PR are presented here. Behaviors of observables such as mean energy, density ρ, and magnetization M (shown in Fig. 10) were found to be either size independent or to depend slightly on sample sizes in the transition region. Furthermore, for all examined sample sizes, we found abrupt jumps of these observables, taking place over a narrow temperature range, $\Delta T=0.0005$.

In Table IV we present the transitional properties such as jumps in mean energy per site and density, respectively, as well as magnetization in the ordered phase, at the first-order phase transition undergone by the three-dimensional PR and He; these results were obtained via MC, MF, and TSC. Comparison shows that TSC produces a better estimate than MF for the transition temperature; on the other hand, MF better predicts the jumps of thermodynamic quantities at the transition. In general, according to the results gathered in Table III, one can see that the phase diagram predicted by the approximate molecular field theories is at least qualitatively correct. This fact is confirmed by the recent simulation results for the phase diagram of the diluted PR reported in Ref. 4.

The susceptibility, actually χ_1, reported in Fig. 11, showed a peak at a temperature about 0.792, a strong sample size dependence below this temperature, and no sensitivity to the sample sizes above it. The behaviors of the three derivatives $C_{\mu V}, \rho_T, \rho_\mu$ (not reported) were found to be *qualitatively* similar to Fig. 6.

Other fluidlike quantities such as R_{JK} (Fig. 12) and R^*_{oo} (not reported here) show how the density behaves when the three-dimensional PR lattice gas model exhibits a first-order transition. These quantities are discontinuous at the transition temperature and follow the behavior obtained for the density and the mean energy; once more we witnessed the smallness

TABLE III. Transition temperatures Θ and "critical" particle density ρ_c of PR and He models for some selected values of the chemical potential μ. Depending on μ, there is either a second-order transition (II) or a first-order transition (I); ρ_c denotes the density at the second-order transition temperature.

Model	μ	Transition	Θ	ρ_c
PR($n=2$)	∞	II	2.201±0.003	1.0
	0.1	II	1.423±0.003	0.6900±0.004
	−1.5	I	0.794±0.001	
He($n=3$)	∞	II	1.443±0.001 (Ref. 36)	1.0
	0.0	II	0.998±0.001 (Ref. 5)	0.743±0.002
	−1.5	I	0.557±0.001	

TABLE IV. Estimates for some properties at first-order transition for the three-dimensional PR and He obtained by different approaches. The results are obtained with $\mu=-1.5$.

Model	Method	Θ	ΔH	$\Delta\rho$	M
PR	MC	0.794±0.001	0.910±0.004	0.684±0.002	0.772±0.002
	MF	0.741	1.138	0.849	0.897
	TSC	0.760	1.518	0.756	0.903
He	MC	0.557±0.001	0.882±0.003	0.877±0.001	0.804±0.001
	MF	0.462	0.944	0.958	0.9126
	TSC	0.482	0.959	0.786	0.888

of the excess quantities R_{oo} due to the absence of purely positional interaction. In general we have remarked a pronounced qualitative similarity between the behaviors of the fluidlike quantities in the present case and those discussed in the preceding section for 2D models.

IV. CONCLUDING REMARKS

We have studied the critical properties of four LG models defined by $\mu<0$ and sufficiently large in magnitude, $\mu=-D/2$, plus an additional case ($D=2$, PR, $\mu=-3D/4$). This allowed us to investigate the impact of the chemical potential on the nature of the phase transition of these models and thus to gain insight into their phase diagrams. Our simulations were performed in the absence of pure positional interaction. A number of thermodynamic quantities including some characteristics of fluid systems were estimated. It was found that the common feature of most cases is the onset of a first-order phase transition induced by the ferromagnetic interaction, and where an abrupt change in the density of the system was observed.

In two dimensions we have investigated both PR and XY models for $\mu=-D/2$. At this value of the chemical potential they showed different critical behaviors. PR exhibited a BKT phase transition, while XY showed a first order one. This might be a consequence of the fact that the two models entail different anchorings with respect to the horizontal plane in spin space. PR was further studied for $\mu=-3D/4$, where evidence of a first-order transition was found. The change of the nature of the phase transition from BKT to a discontinuous one agrees with previous RG predictions[23,24] and rigorous mathematical results;[22] on the other hand, in recent simulation studies of quenched dilution it was found that the transition temperature vanishes below the percolation threshold.[28–31]

Notice that usage of the grand-canonical ensemble allows quite wide changes of density with temperature. Such changes are obviously excluded from the start in the treatment of a quenched-dilution model. Thus, there are significant differences between both methods, yet the two resulting pictures are somehow compatible.

Phase transition and critical dynamics in site-diluted arrays of Josephson junctions were recently studied experimentally in Ref. 41; according to the results of Yun *et al.*, the BKT transition is altered by the introduction of percolative disorder far below the percolation threshold. Furthermore, the authors of Ref. 41 found evidence of a non-BKT-type superconducting transition for strongly disordered samples, taking place at finite temperature. Our results suggest that the transition in the named region becomes of first order.

For the three-dimensional models investigated here, i.e., PR and He, we found a first-order phase transition form a

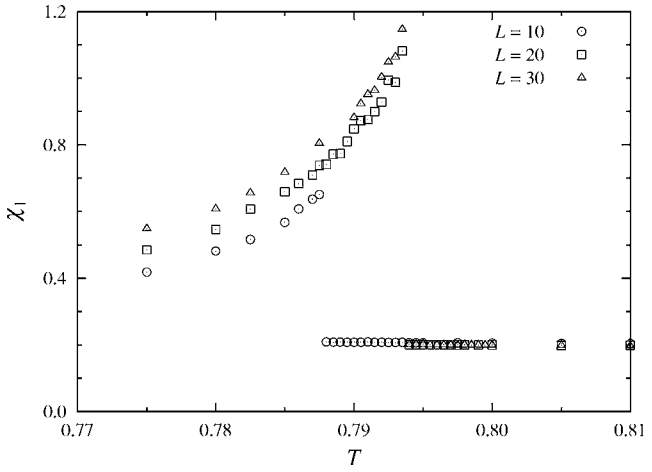

FIG. 11. Simulation results for the susceptibility χ_1 for the three-dimensional LG-PR, obtained with different sample sizes. The associated statistical errors, not shown, range up to 10%. The value $\mu=-1.5$ was used in this simulation.

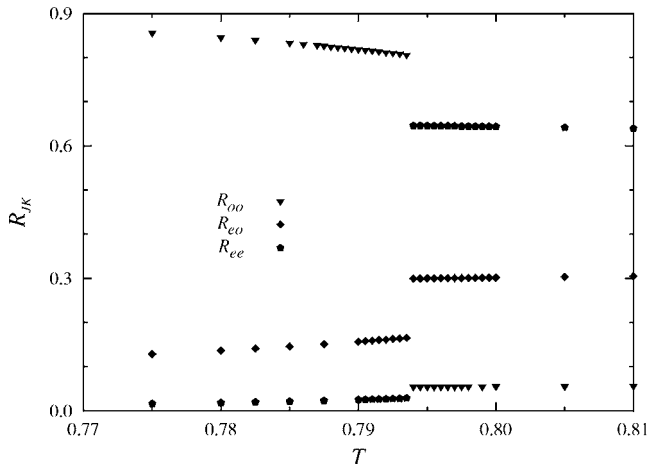

FIG. 12. Simulation results for the three pair occupation probabilities R_{JK} obtained for the three-dimensional LG-PR with linear sample size $L=30$. The value $\mu=-1.5$ was used in this simulation.

ferromagnetic dense phase to a diluted paramagnetic one. The results obtained via simulation for $\mu=-D/2$ were found to confirm those obtained by molecular field approximations used to construct the phase diagram of Refs. 3 and 5, showing that the phase diagrams obtained there are qualitatively correct.

ACKNOWLEDGMENTS

The present calculations were carried out on, among other machines, workstations belonging to the Sezione di Pavia of INFN (Istituto Nazionale di Fisica Nucleare). Allocation of computer time by the Computer Centre of Pavia University and CILEA (Consorzio Interuniversitario Lombardo per l' Elaborazione Automatica, Segrate-Milan), as well as by CINECA (Centro Interuniversitario Nord-Est di Calcolo Automatico, Casalecchio di Reno-Bologna), are gratefully acknowledged as well. One of the authors (H.C.) also acknowledges financial support from Grant No. BK6/2007 of ISSP-BAS. The authors also thank V. A. Zagrebnov (CPT-CNRS and Université de la Méditerranée, Luminy, Marseille, France) and A. C. D. van Enter (Rijksuniversiteit Groningen, the Netherlands) for helpful discussions.

[1] S. Romano, Int. J. Mod. Phys. B **13**, 191 (1999).
[2] R. O. Sokolovskii, Phys. Rev. B **61**, 36 (2000).
[3] S. Romano and R. O. Sokolovskii, Phys. Rev. B **61**, 11379 (2000).
[4] A. Maciołek, M. Krech, and S. Dietrich, Phys. Rev. E **69**, 036117 (2004).
[5] H. Chamati and S. Romano, Phys. Rev. B **72**, 064424 (2005).
[6] H. Chamati and S. Romano, Phys. Rev. B **72**, 064444 (2005).
[7] R. T. S. Freire, S. J. Mitchell, J. A. Plascak, and D. P. Landau, Phys. Rev. E **72**, 056117 (2005).
[8] H. Chamati and S. Romano, Phys. Rev. B **73**, 184424 (2006).
[9] Ya. G. Sinaĭ, *Theory of Phase Transitions; Rigorous Results* (Pergamon, Oxford, 1982).
[10] H.-O. Georgii, *Gibbs Measures and Phase Transitions* (de Gruyter, Berlin, New York, 1988).
[11] P. Bruno, Phys. Rev. Lett. **87**, 137203 (2001).
[12] A. Pelissetto and E. Vicari, Phys. Rep. **362**, 549 (2002).
[13] M. E. J. Newman and G. T. Barkema, *Monte Carlo Methods in Statistical Physics* (Clarendon, Oxford, 1999).
[14] S. Romano and V. A. Zagrebnov, Physica A **253**, 483 (1998).
[15] N. Angelescu and V. A. Zagrebnov, J. Phys. A **15**, L639 (1982).
[16] N. Angelescu, S. Romano, and V. A. Zagrebnov, Phys. Lett. A **200**, 433 (1995).
[17] V. A. Zagrebnov, Physica A **232**, 737 (1996).
[18] L. Chayes, S. B. Shlosman, and V. A. Zagrebnov, J. Stat. Phys. **98**, 537 (2000).
[19] J. Fröhlich and T. Spencer, Commun. Math. Phys. **81**, 527 (1981).
[20] Z. Gulácsi and M. Gulácsi, Adv. Phys. **47**, 1 (1998).
[21] C. Gruber, H. Tamura, and V. A. Zagrebnov, J. Stat. Phys. **106**, 875 (2002).
[22] A. C. D. van Enter, S. Romano, and V. A. Zagrebnov, J. Phys. A **39**, L439 (2006).
[23] J. L. Cardy and D. J. Scalapino, Phys. Rev. B **19**, 1428 (1979).
[24] A. N. Berker and D. R. Nelson, Phys. Rev. B **19**, 2488 (1979).
[25] I. P. Omelyan, I. M. Mryglod, R. Folk, and W. Fenz, Phys. Rev. E **69**, 061506 (2004).
[26] Yu. E. Lozovik and L. M. Pomirchy, Solid State Commun. **89**, 145 (1994).
[27] L. M. Castro, A. S. T. Pires, and J. A. Plascak, J. Magn. Magn. Mater. **248**, 62 (2002).
[28] S. A. Leonel, P. Zimmermann Coura, A. R. Pereira, L. A. S. Mól, and B. V. Costa, Phys. Rev. B **67**, 104426 (2003).
[29] B. Berche, A. I. Fariñas-Sánchez, Yu. Holovatch, and R. Paredes V, Eur. Phys. J. B **36**, 91 (2003).
[30] T. Surungan and Y. Okabe, Phys. Rev. B **71**, 184438 (2005).
[31] G. M. Wysin, A. R. Pereira, I. A. Marques, S. A. Leonel, and P. Z. Coura, Phys. Rev. B **72**, 094418 (2005).
[32] M. P. Allen and D. J. Tildesley, *Computer Simulation of Liquids* (Oxford University Press, Oxford, UK, 1989).
[33] S. Romano, Int. J. Mod. Phys. B **9**, 85 (1995).
[34] R. Hashim and S. Romano, Int. J. Mod. Phys. B **13**, 3879 (1999).
[35] Th. T. A. Paauw, A. Compagner, and D. Bedaux, Physica A **79**, 1 (1975).
[36] P. Peczak, A. M. Ferrenberg, and D. P. Landau, Phys. Rev. B **43**, 6087 (1991).
[37] J. Tobochnik and G. V. Chester, Phys. Rev. B **20**, 3761 (1979).
[38] S. Romano, Int. J. Mod. Phys. B **16**, 2901 (2002).
[39] S. Romano, Physica A **324**, 606 (2003).
[40] P. Archambault, S. T. Bramwell, and P. C. W. Holdsworth, J. Phys. A **30**, 8363 (1997).
[41] Y.-J. Yun, I.-C. Baek, and M.-Y. Choi, Phys. Rev. Lett. **97**, 215701 (2006).